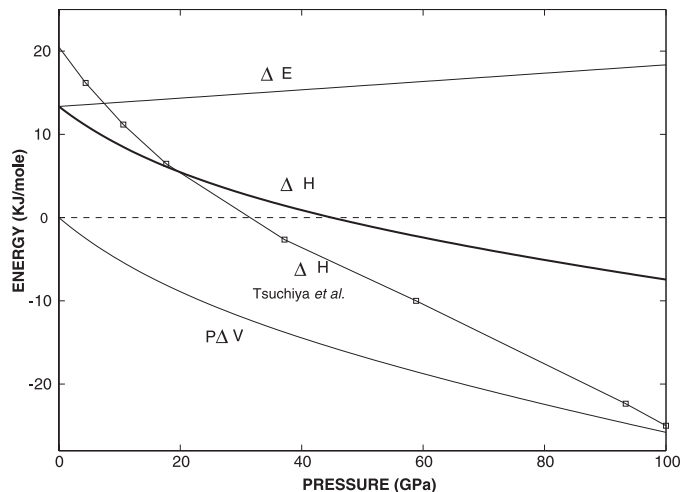**Fig. 4.** HS-to-LS transition enthalpy, $\Delta H = \Delta E + P\Delta V$, and component terms, ΔE and $P\Delta V$. The thick solid line showing the enthalpy was obtained from the data of Lin *et al.* (*11*) (see text). It is a sum of the individual components shown. The line with squares is the result of a first-principles calculation by Tsuchiya *et al.* (*15*).

We have measured the elastic tensor of $(Mg_{0.94},Fe_{0.06})O$ through the pressure-induced HS-to-LS transition. We find that there is an extensive range of pressure over which all the c_{ij} exhibit an anomalous but smooth softening. By reinterpreting previously published compression data of materials with much higher iron concentrations (more representative of the lower mantle), we show that similar but even more pronounced behavior is exhibited by at least the bulk modulus. The current data show that, even at room temperature, the HS-to-LS transition in (Mg,Fe)O is not expected to result in a sudden increase in seismic velocities at any depth. Although this finding is inconsistent with the conclusions of (*11*), it is qualitatively consistent with the results of the more recent x-ray emission experiment carried out at simultaneous high pressure and temperature by Lin *et al.* (*17*), who noted that the spin transition takes place over an extended range of pressure and temperature. On the basis of our room-temperature results, this range extends from 1000 to 1500 km. At elevated temperatures and on the basis of Eq. 1, this range increases to include most or all of the lower mantle and results in a decrease in compressional and shear velocities of a few percent.

References and Notes

1. E. Ito, E. Takahashi, *J. Geophys. Res.* **94**, 10637 (1989).
2. T. Irifune *et al.*, *Science* **279**, 1698 (1998).
3. C. R. Bina, *Rev. Mineral. Geochem.* **37**, 205 (1998).
4. S. E. Kesson, J. D. Fitz Gerald, H. St. C. O'Neill, J. M. G. Shelley, *Phys. Earth Planet. Inter.* **131**, 295 (2002).
5. Y. Fei, *Rev. Mineral. Geochem.* **37**, 343 (1998).
6. D. Andrault, *J. Geophys. Res.* **106**, 2079 (2001).
7. J. Badro *et al.*, *Science* **300**, 789 (2003).
8. M. Murakami, K. Hirose, N. Sata, Y. Ohishi, *Geophys. Res. Lett.* **32**, L03304 (2005).
9. Y. Kobayashi *et al.*, *Geophys. Res. Lett.* **32**, L19301 (2005).
10. S. Speziale *et al.*, *Proc. Natl. Acad. Sci. U.S.A.* **102**, 17918 (2005).
11. J. F. Lin *et al.*, *Nature* **436**, 377 (2005).
12. J. F. Lin *et al.*, *Geophys. Res. Lett.* **33**, L22304 (2006).
13. A. F. Goncharov, V. V. Stuzhkin, S. D. Jacobsen, *Science* **312**, 1205 (2006).
14. W. Sturhahn, J. M. Jackson, J. F. Lin, *Geophys. Res. Lett.* **32**, L12307 (2005).
15. T. Tsuchiya, R. M. Wentzcovitch, C. R. S. da Silva, S. de Gironcoli, *Phys. Rev. Lett.* **96**, 198501 (2006).
16. H. Persson, A. Bengtson, G. Ceder, D. Morgan, *Geophys. Res. Lett.* **33**, L16306 (2006).
17. J. F. Lin *et al.*, *Science* **317**, 1740 (2007).
18. Materials and methods are available as supporting material on *Science* Online.
19. J. M. Jackson *et al.*, *J. Geophys. Res.* **111**, 09203 (2006).
20. Acoustic velocities and moduli are tabulated in tables S1 and S2. Figure S1 presents the inferred aggregate shear modulus as a function of pressure.
21. Y. Fei *et al.*, *Geophys. Res. Lett.* **34**, L17307 (2007).
22. Parameters for the HS phase are $K_0 = 158$ GPa, $K' = 4.0$, and $K'' = 0$, with $\rho_0 = 3.994$ g cm^{-3} (where K_0, K', K'', and ρ_0 are the bulk modulus, the first and second derivatives of the bulk modulus, and the density at zero pressure). For the LS phase, they are $K_0 = 185$ GPa, $K' = 3.90$, and $K'' = 0$, with $\rho_0 = 4.221$ g cm^{-3}.

Enriched Pt-Re-Os Isotope Systematics in Plume Lavas Explained by Metasomatic Sulfides

Ambre Luguet,[1]*† D. Graham Pearson,[1] Geoff M. Nowell,[1] Scott T. Dreher,[1] Judith A. Coggon,[1] Zdislav V. Spetsius,[2] Stephen W. Parman[1]

To explain the elevated osmium isotope (^{186}Os-^{187}Os) signatures in oceanic basalts, the possibility of material flux from the metallic core into the crust has been invoked. This hypothesis conflicts with theoretical constraints on Earth's thermal and dynamic history. To test the veracity and uniqueness of elevated ^{186}Os-^{187}Os in tracing core-mantle exchange, we present highly siderophile element analyses of pyroxenites, eclogites plus their sulfides, and new ^{186}Os/^{188}Os measurements on pyroxenites and platinum-rich alloys. Modeling shows that involvement in the mantle source of either bulk pyroxenite or, more likely, metasomatic sulfides derived from either pyroxenite or peridotite melts can explain the ^{186}Os-^{187}Os signatures of oceanic basalts. This removes the requirement for core-mantle exchange and provides an effective mechanism for generating Os isotope diversity in basalt source regions.

The possibility of observing the chemical signature of core-mantle interaction in magmas erupted at Earth's surface is one of the most exciting prospects in mantle geochemistry. The observation of ^{186}Os/^{188}Os-^{187}Os/^{188}Os excesses in some plume-related lavas has recently been invoked as the strongest evidence of substantial mass exchange between the Earth's core and mantle (*1–5*). This hypothesis has considerable consequences for the evolution of the core, specifically requiring inner core crystallization early in Earth's history. This constraint on the inner core's crystallization age is in direct con-

tradiction of recent models of terrestrial cooling (*6, 7*) which predict ages of core crystallization as young as 1.5 billion years (Gy) old, too late then to generate the required ^{186}Os enrichment. Further objections to the core-mantle exchange model have come from the absence of ϵ^{182}W anomalies in the same plume-related lavas (*8*) and from new high-pressure solid metal–liquid metal highly siderophile element (HSE) partition coefficients (*9*), which predict an outer core composition that is unable to generate elevated ^{186}Os and ^{187}Os, even over several billion years (Fig. 1). With the continued finding of ^{186}Os/^{188}Os-^{187}Os/^{188}Os

excesses in mantle-derived magmas, it is timely to examine other potential explanations of this signature to find a possible resolution of these contradictions.

Recycling of crustal materials such as Fe-Mn crusts, oceanic crust, or melting of a mixed pyroxenite-peridodite source (10–12) have been proposed instead of core-mantle interaction. These alternative hypotheses focus on intramantle mixing processes and have considerably different implications for the thermal and dynamic evolution of Earth. They each have weaknesses. Recycling of Fe-Mn crusts and oceanic crust were ruled out because of their variable [187]Os signature, their volumetrically low abundance, and their low Os contents (1). The mixed pyroxenite-peridodite source hypothesis is more attractive but has not been properly tested with a representative, extensive Re-Pt-Os abundance and isotopic database. Nonetheless, this hypothesis is in accord with recent geochemical and petrological studies that involve large contributions (10 to 100%) of pyroxenite-derived melts in the source of mid-ocean ridge basalts, ocean island basalts, and komatiites (13, 14). Hence, more detailed documentation of pyroxenite HSE abundances and Os isotope systematics is required, especially the potential role of base-metal sulfides (BMS) in generating highly variable [186]Os-[187]Os isotope systematics in prospective basalt source regions. BMS control the HSE abundance budget of the mantle [e.g., (15)]. These minerals are highly mobile in the mantle, being capable of metasomatizing mantle sources (15–17). They can then introduce a wide variety of Os isotope compositions and Pt/Os and Re/Os fractionations (15–17). As such, BMS may hold the key to understanding mantle [186]Os-[187]Os isotope systematics.

We report [186]Os/[188]Os and [187]Os/[188]Os compositions (calculated and measured) together with HSE abundances for 11 pyroxenites from the Beni Bousera orogenic massif (table S1) (18). In addition, 20 BMS grains have also been measured from Beni Bousera pyroxenites plus eclogite xenoliths from the Mir and Udachnaya kimberlites. Beni Bousera pyroxenites are considered to be good analogs of pyroxenites present within the asthenospheric mantle because they appear to be derived from an oceanic crust protolith (19). They have reaction margins with the surrounding peridotites that are analogs for the hybrid sources required by melts with a substantial pyroxenite influence (20). Eclogite xenoliths have also been shown to have a recycled crustal origin (21) and have experienced long-term residence in the lithospheric mantle (22).

[1]Northern Centre for Isotopic and Elemental Tracing, Department of Earth Sciences, University of Durham, South Road, Durham DH1 3LE, UK. [2]Yakutian Research and Design Institute of Diamond Mining Industry, ALROSA Joint-Stock Company, Mirny, Yakutia 678170, Russia.

*Present address: Mineralogisch-Petrologisches Institut, Universität Bonn, Poppelsdorfer Schloss, 53115 Bonn, Germany. †To whom correspondence should be addressed. E-mail: ambre.luguet@durham.ac.uk

Sulfides from these lithologies provide the host for most of the Os signatures and together with their low melting points provide an effective means of transferring Os isotope signatures. Because of difficulties in obtaining sufficient Os for precise analysis of [186]Os/[188]Os ratios, especially in single mantle-derived sulfides, we model most of the [186]Os/[188]Os compositions by assuming an age for the pyroxenites of 1.2 Gy (18). This age is indicated for some Beni Bousera pyroxenites by a previous Lu-Hf and Re-Os study (19). Although ancient, the 1.2-Gy age is somewhat younger than the suggested mean age of recycled oceanic crust residing in the convecting mantle on the basis of Pb isotopes (23). As such, the ranges of isotopic compositions that we report are likely conservative minima (18).

Beni Bousera pyroxenites show pronounced but very variable enrichment of Pt and Re over Os (Fig. 1). Their calculated (C) [187]Os/[188]Os$_C$ ratios (18) are systematically radiogenic. Their [186]Os/[188]Os$_C$ ratios vary over a wide range, from close to chondritic to considerably radiogenic ([186]Os/[188]Os$_C$ = 0.1198401 to 0.1198934). The most radiogenic [186]Os/[188]Os$_C$ ratios are substantially higher than the most radiogenic plume-related lava sample (Fig. 1). The measured (M) [187]Os/[188]Os$_M$ and [186]Os/[188]Os$_M$ ratios obtained for GP137 and GP251, two samples where sufficient whole-rock powder was available for anal-

ysis, confirm our calculations. In particular, GP 137 has a nonradiogenic [186]Os/[188]Os$_M$ signature, whereas GP 251 is radiogenic in [186]Os, even more so than are plume-related lavas (ε[186]Os = +0.71, compared to the most radiogenic Gorgona samples). The slight discrepancy observed between the measured and calculated isotopic ratios likely reflects the variable, inherited, radiogenic Os in the pyroxenite at the time of their formation because the Beni Bousera pyroxenites have an origin from recycled oceanic crust.

The isotopic diversity of the pyroxenites makes them attractive as potential source components for explaining lavas' [186]Os-[187]Os systematics. Partial melts derived from a mantle source containing both peridotites and pyroxenites similar in HSE composition to those at Beni Bousera could reproduce the radiogenic Os isotopic composition of plume-related lavas (Fig. 2). A simple two-component bulk mixing model calculated between a present-day mantle peridotite and the two pyroxenites with the highest [186]Os/[188]Os (GP 251 and GP 87T) indicates that a basalt containing 50 to 90% of pyroxenite-derived melt would have combined [187]Os/[188]Os and [186]Os/[188]Os ratios similar to the radiogenic plume-related lavas. More specifically, our calculations indicate that 60%, 70 to 75%, and 85% of pyroxenite-derived melts could explain the [186]Os-[187]Os systematics of Mauna Loa, Loihi,
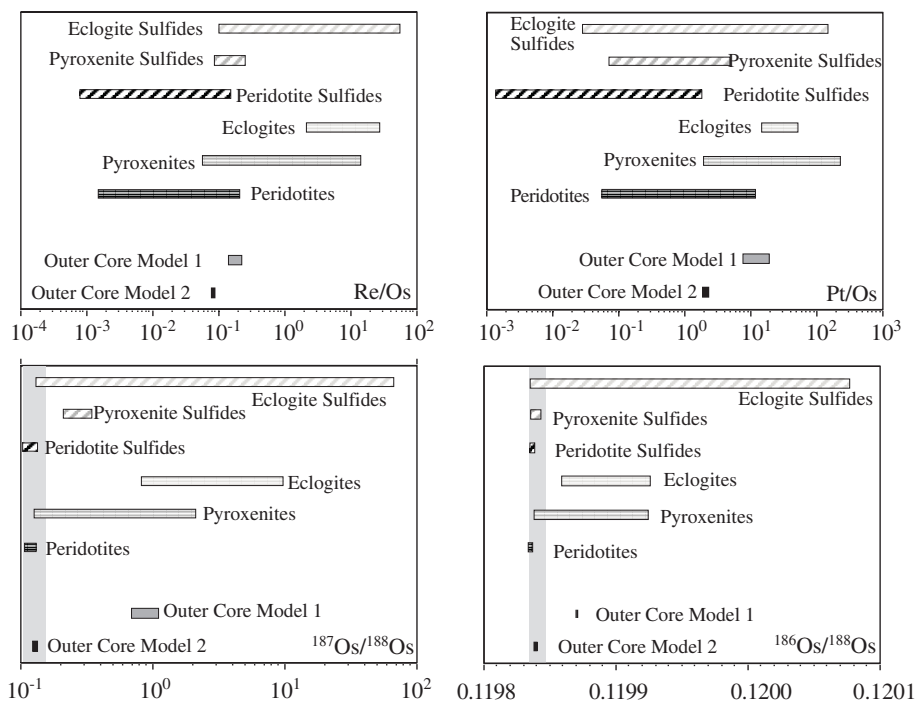

Fig. 1. Variations of Re/Os, Pt/Os, [187]Os/[188]Os, and [186]Os/[188]Os for models of the outer core compared with measured and predicted values for whole-rock peridotites (15, 16, 29), eclogites (22), pyroxenites (table S1) (19), sulfides from eclogites and pyroxenites (table S1), and residual sulfides from peridotites (15–17). The gray field denotes Os isotopic composition of [186]Os-enriched plume-related lavas (2–5). The outer core model 1 is from (4) and assumes a 4.4- to 3.4-Gy-old inner core. The outer core model 2 was calculated using bulk core composition of (4), Os, Ir, and Pt metal solid/metal liquid partition coefficients experimentally obtained at 22-Gy (9) and a 1.5-GPa crystallization age of the inner core in agreement with Earth heat budgets (6, 7). Outer core model calculations were performed assuming both linear and instant growth models for the inner core crystallization.

and Hualalai shield volcanoes, respectively, in good agreement with the estimates made using ^{187}Os-^{87}Sr systematics (13). These large volumes of pyroxenite-derived melts imply 4 to 16% of recycled crust within the mantle source (14), in excellent agreement with the proportion of pyroxenitic material observed in subcontinental lithospheric mantle and ophiolite massifs (5 to 10% volume) (19).

Although the above estimates of the proportion of pyroxenite in the source of mantle-derived magmas, made on the basis of Pt-Re-Os isotope systematics, are consistent with the proportions indicated from other constraints (13, 14), bulk mixing models are probably not applicable to mass balance arguments involving HSE. This is because these elements are concentrated within BMS which, during melting and mixing processes, will not behave like silicate phases. Being highly reactive and mobile trace components of mantle rocks (15–17), BMS have the ability to produce dramatic changes in HSE abundances and isotopic ratios during metasomatic events where very low mass fractions are exchanged, principally the low-temperature melting components such as BMS.

In mantle peridotites, HSE contents and ^{187}Os/^{188}Os ratios of the BMS vary largely at the micrometric scale (15–17) (Fig. 1). That this microscale heterogeneity extends to the pyroxenitic/eclogitic parageneses is confirmed by the wide range of HSE concentrations with Re/Os and Pt/Os ratios, spanning 0.5 to 3 orders of magnitude, within BMS from Beni Bousera pyroxenites and Udachnaya and Mir eclogites (table S1 and Fig. 1). However, in contrast to peridotite sulfides, pyroxenite and eclogite BMS systematically have radiogenic to very radiogenic ^{187}Os$_C$ compositions (Fig. 1). Half the samples show subchondritic to slightly suprachondritic ^{186}Os/^{188}Os$_C$ ratios (0.1198369 to 0.1198454) (table S1), whereas the rest have very radiogenic to extreme ^{186}Os/^{188}Os$_C$ ratios (0.1198557 to 0.1200785). The most radiogenic ^{186}Os/^{188}Os$_C$

ratios are considerably higher than the whole-rock pyroxenites or eclogites and well in excess of any modeled outer core compositions (Fig. 1). ^{186}Os/^{188}Os ratios even more extreme than the BMS values modeled here have been measured in Pt-rich alloys from ophiolites (up to 0.1217) (table S1) (11), confirming the potential of HSE carriers to generate highly radiogenic signatures within the shallow upper mantle.
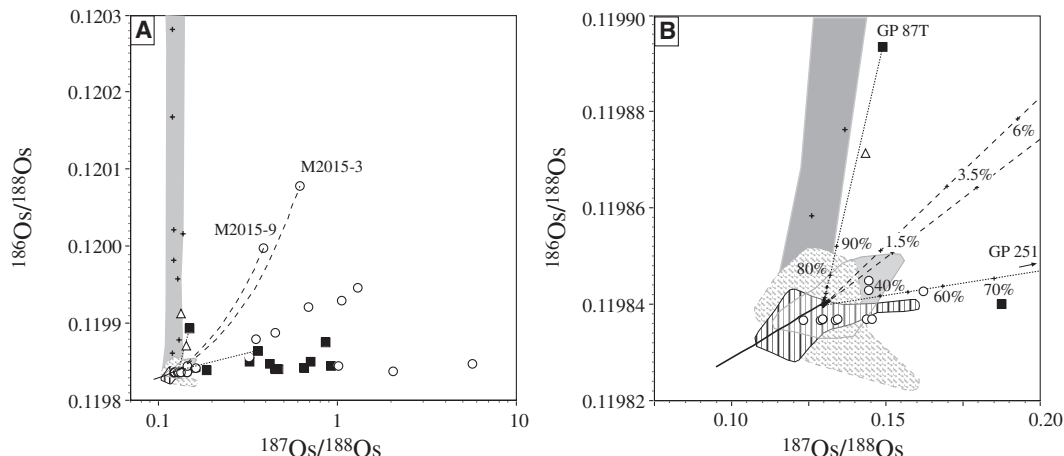
During melting of a mixed pyroxenite-peridotite source, the pyroxenitic component melts first, with the resulting melts reacting with the peridotite wall-rocks (20). It is this reacted wall-rock that subsequently controls melt composition. During this process, sulfides, because of their low solidi, will be among the first components to be transferred into the surrounding metasomatized wall-rock. Melting of mantle peridotite that has been metasomatically enriched with HSE-rich, isotopically heterogeneous microphases such as BMS derived from pyroxenites or eclogites could explain the entire spectrum of ^{187}Os-^{186}Os variation in plume-related lavas (Fig. 2). For example, melting of a peridotitic mantle containing 1.5% of BMS similar to the two eclogite BMS M2015-3 and M2015-9, would generate partial melt with an Os isotopic composition matching the most radiogenic Gorgona komatiite samples. The amount of metasomatic BMS required is as low as 0.035 to 0.12% if the BMS are Os-rich, such as those observed in some highly metasomatized peridotites from the Kaapvaal craton (24) (e.g., FRB 98/6). Of course, the proportion of metasomatic sulfides is highly dependent on the assumptions made to model their Os isotopic composition. For example, the proportion of sulfides required for the mass balance is multiplied by a factor of 2 to 3 if sulfides are 500 million years (My) old but drop by a factor of 2 if the sulfides are 2 Gy old. Moreover, although the reacted peridotite composition is likely to be affected by the addition of metasomatic sulfides, especially regarding S and Pt contents (18), the oceanic basalts are unlikely

to inherit those anomalous signatures because of the limited solubility of these two elements within silicate melts (25, 26).

HSE alloys are a possible alternative to BMS being the key agent for dominating the ^{187}Os-^{186}Os source characteristics of magma source regions. HSE alloys can have extremely radiogenic ^{186}Os/^{188}Os and ^{187}Os/^{188}Os and high HSE contents (Fig. 2 and table S1) (11). Although these mostly form in the oceanic mantle lithosphere (11, 27), their very radiogenic values, such as those found here, can be explained by in-growth during crustal residence. Nonetheless, if such grains found their way back into mantle source regions through recycling of lithosphere, they are likely to dominate mantle HSE budgets and isotope systematics. Although the potential of transferring their Os isotopic signatures to partial melts is unclear because of their refractory and chemically inert nature, HSE alloy recycling in the mantle could represent another potential mechanism to diversify the Os isotopic composition of upper-mantle–derived melts worthy of further research.

We conclude that the coupled ^{186}Os-^{187}Os enrichment observed in plume-related lavas can have an upper-mantle origin related to source regions having experienced BMS metasomatism by pyroxenite and/or peridotite-derived partial melts. Addition of metasomatic sulfides to mantle peridotite is a common process in the lithospheric mantle. It has been shown to operate also in the oceanic mantle, explaining both the ^{187}Os/^{188}Os systematics of abyssal peridotites (17) and the Pd enrichment of the oceanic mantle (15, 16). Sulfide metasomatism, and its resulting effects on S abundances, has been documented in veined pyroxenite-peridotite sequences (28), and the measurements and modeling presented here illustrate the effectiveness of the process in dominating the ^{186}Os-^{187}Os systematics of mantle rocks. Hence, the observation of coupled ^{186}Os-^{187}Os excesses in mantle-derived magmas cannot be taken to be a unique signature of core-mantle interaction.

Fig. 2. (A) ^{186}Os-^{187}Os systematics of Beni Bousera pyroxenites (squares, predicted), sulfides from pyroxenite and eclogite sulfides (circles, predicted), Kaapvaal peridotites (triangles, predicted) (24), and HSE alloys from the Josephine ophiolite (dark gray field and crosses, measured). The medium gray field denotes plume-related lavas (2–5); obliquely lined field, osmiridiums (11); and vertically lined field, osmiridiums and chromitites (2, 30). The dotted line represents the mixing line between pyroxenites GP87T and GP251 and a present-day mantle peridotite, and the dashed lines represent the mixing

line between the eclogite sulfides (M2015-3 and M2015-9) and a present-day mantle peridotite. Mass of sulfides in mixture denoted in %. **(B)** is a magnification of (A) to better show the match between ^{186}Os-enriched plume-related lavas and the metasomatic sulfides to peridotite mixing trend. The x axis in (A) is in logarithmic units.

References and Notes

1. A. D. Brandon, R. J. Walker, *Earth Planet. Sci. Lett.* **232**, 211 (2005).
2. R. J. Walker *et al.*, *Geochim. Cosmochim. Acta* **61**, 4799 (1997).
3. A. D. Brandon, M. D. Norman, R. J. Walker, J. W. Morgan, *Earth Planet. Sci. Lett.* **174**, 25 (1999).
4. A. D. Brandon *et al.*, *Earth Planet. Sci. Lett.* **206**, 411 (2003).
5. I. S. Puchtel, A. D. Brandon, M. Humayun, R. J. Walker, *Earth Planet. Sci. Lett.* **237**, 118 (2005).
6. S. Labrosse, J.-P. Poirier, J.-L. Le Mouel, *Earth Planet. Sci. Lett.* **190**, 111 (2001).
7. F. Nimmo, G. D. Price, J. Brodholt, D. Gubbins, *Geophys. J. Int.* **156**, 363 (2004).
8. A. Schersten, T. Elliot, C. Hawkesworth, M. Norman, *Nature* **427**, 234 (2004).
9. J. A. Van Orman, S. Keshav, Y. Fey, *Geochim. Cosmochim. Acta* **70**, A666 (2006).
10. J. A. Baker, K. K. Jensen, *Earth Planet. Sci. Lett.* **220**, 277 (2004).
11. A. Meibom, R. Frei, N. H. Sleep, *J. Geophys. Res.* **109**, B02203 10.1029/2003JB002602 (2004).
12. A. D. Smith, *J. Geodynamics* **36**, 469 (2003).
13. A. V. Sobolev, A. W. Hofmann, S. V. Sobolev, I. K. Nikogosian, *Nature* **434**, 590 (2005).
14. A. V. Sobolev *et al.*, *Science* **316**, 412 (2007).
15. A. Luguet *et al.*, *Earth Planet. Sci. Lett.* **189**, 285 (2001).
16. A. Luguet, J.-P. Lorand, O. Alard, J.-L. Cottin, *Chem. Geol.* **208**, 175 (2004).
17. O. Alard *et al.*, *Nature* **436**, 1005 (2005).
18. Information on material and methods are available as supporting material on *Science* Online.
19. D. G. Pearson, G. M. Nowell, *J. Petrol.* **45**, 439 (2004).
20. G. M. Yaxley, D. H. Green, *Schweiz. Mineral. Petrogr. Mitt.* **78**, 243 (1998).
21. I. D. MacGregor, W. I. Manton, *J. Geophys. Res.* **91**, 14063 (1986).
22. D. G. Pearson *et al.*, *Geochim. Cosmochim. Acta* **59**, 959 (1995).
23. A. W. Hofmann, in *Treatise on Geochemistry, Vol. 2, The Mantle and Core*, H. D. Holland, K. K. Turekian, Eds., pp. 61–101 (2004).
24. W. L. Griffin, S. Graham, S. Y. O'Reilly, N. J. Pearson, *Chem. Geol.* **208**, 89 (2004).
25. J. A. Mavrogenes, H. St. C. O'Neill, *Geochim. Cosmochim. Acta* **63**, 1173 (1999).
26. A. Borisov, H. Palme, *Am. Mineral.* **85**, 1665 (2000).
27. D. G. Pearson, S. W. Parman, G. M. Nowell, *Nature* **449**, 202 (2007).
28. J.-P. Lorand, *J. Petrol.* **30**, 987 (1989).
29. D. G. Pearson, G. J. Irvine, D. A. Ionov, F. R. Boyd, G. E. Dreibus, *Chem. Geol.* **208**, 29 (2004).
30. R. J. Walker *et al.*, *Earth Planet. Sci. Lett.* **230**, 211 (2005).
31. We thank R. W. Carlson and J.-P. Lorand for fruitful discussions and two anonymous reviewers for their constructive comments. A.L. thanks the European Community for the Marie Curie postdoctoral fellowship (EIF-ENV-009752) during which this work was done. The instrumentation used in this study was supported by Natural Environment Research Council (NERC)/Higher Education Funding Council for England (HEFCE) grant JREI JRDUPEEQ.

Irreconcilable Differences: Fine-Root Life Spans and Soil Carbon Persistence

Allan E. Strand,[1] Seth G. Pritchard,[1]* M. Luke McCormack,[2] Micheal A. Davis,[3] Ram Oren[4]

The residence time of fine-root carbon in soil is one of the least understood aspects of the global carbon cycle, and fine-root dynamics are one of the least understood aspects of plant function. Most recent studies of these belowground dynamics have used one of two methodological strategies. In one approach, based on analysis of carbon isotopes, the persistence of carbon is inferred; in the other, based on direct observations of roots with cameras, the longevity of individual roots is measured. We show that the contribution of fine roots to the global carbon cycle has been overstated because observations of root lifetimes systematically overestimate the turnover of fine-root biomass. On the other hand, isotopic techniques systematically underestimate the turnover of individual roots. These differences, by virtue of the separate processes or pools measured, are irreconcilable.

Fine roots (those with diameters <2.0 mm) serve at least two roles of global importance: They act as conduits transporting carbon (C) into belowground C pools, and they acquire soil resources. Consequently, predictive models of plant function, forest nutrition, and global C cycling depend on accurate quantification of fine-root longevity and turnover rate.

Considerable effort has been expended to quantify the potential for fine roots to absorb C from the growing pool of atmospheric CO_2 and to sequester it in mineral soil. Globally, soil C pools are particularly important because they contain approximately 3.3 times more C than the atmospheric pool and 4.0 times more C than the aboveground terrestrial biomass pool (*1–4*). Much of the C present in soil is probably derived from fine roots (*5*).

Understanding fine-root dynamics is also critical for understanding how plants acquire water and nutrients from soil. Because most uptake occurs in roots <1 mm in diameter, fine-root pool size may limit forest productivity by limiting plant absorptive capacity. Fine roots are also the primary site of infection by mycorrhizal fungi, which influence a wide range of ecosystem properties, including productivity, biodiversity, and soil structure.

There is currently an ongoing debate on the efficacy of methods that measure C residence time in fine roots using ^{13}C-depleted atmospheric enrichment (*6*) versus methods that observe roots directly by means of microvideo cameras (minirhizotrons) (*6–8*). This debate has been fueled by the observation that isotope-based estimates of C residence times in fine roots are much longer (>4 years) than estimates of root longevity determined by repeated observation with minirhizotrons (<1 year) (*9, 10*).

Several sources of discrepancy between these approaches have been identified: (i) differences in the pool of roots sampled with isotope versus minirhizotron methods (*8, 11*), (ii) the confounding effects of carbohydrate storage on depletion rates of C isotopes (*12*), (iii) the appropriateness of underlying survival functions assumed by isotope methods (*10, 13*), (iv) overestimation of turnover rate because of using median longevity as a surrogate for mean longevity in minirhizotron studies (*11*), and (v) slow return to equilibrium root dynamics after the installation of minirhizotron access tubes (*14*).

Although technical issues inherent to isotopic and minirhizotron methods have led to disparate conclusions about fine-root dynamics, arguments regarding the validity of these methods skirt the issue that multiple belowground processes require characterization and, although related, may best be measured with different approaches. In this study, we set out to reconcile measures of fine-root C pool dynamics derived with isotopic methods and fine-root dynamics obtained from minirhizotrons. First, we assess the relative magnitudes of several sources of measurement error associated with isotope and minirhizotron approaches; second, we attempt to quantify the differences between C residence and individual root-dynamic–focused studies. We used survival analysis to examine the root dynamics in the CO_2-enriched plots at the Duke University free-air CO_2 enrichment (FACE) facility (*15*). The longevity of 2181 individual roots, with diameters <2 mm, was recorded over 8 years from repeated video images; 64% of these roots were followed until senescence and death. The remainder were alive at the end of the experiment and were treated as right-censored in survival analyses. We then compared our results to estimates of root turnover derived using isotopic techniques from the same forest plots, published by Matamala *et al.* (*6*).

Previously published isotopic estimates of turnover for this forest (*6*) have been criticized on

[1]Department of Biology, College of Charleston, Charleston, SC 29424, USA. [2]Huck Institutes of Life Sciences, The Pennsylvania State University, University Park, PA 16802, USA. [3]Department of Biology, University of Southern Mississippi, Hattiesburg, MS 39406–5018, USA. [4]Nicholas School of the Environment and Earth Sciences, Duke University, Durham, NC 27708, USA.

*To whom correspondence should be addressed. E-mail: pritchards@cofc.edu